To cite this version :

Friction behavior of laser cladding magnesium alloy against AISI 52100 steel

A. Fabre *, J.E. Masse

Arts et Métiers ParisTech, MécaSurf Laboratory, 2, Cours des Arts et Métiers, 13617 Aix-en-Provence, France

ABSTRACT

The use of magnesium alloys in engineering applications is becoming increasingly important as a relatively low density allows savings in energy consumption and therefore reduction in air pollution. An associated reduction in inertia makes these alloys potential candidates for friction components, but they suffer from poor wear resistance. Laser surface alloying with appropriate powder mixture is an innovative technique to improve surface properties of metallic alloys. In this study, the effect of laser surface alloying using Al12%Si powder on wear resistance of a magnesium alloy ZE41 is investigated. Hardness and wear resistance of the alloy are significantly enhanced after treatment.

1. Introduction

The need for weight reduction in the aircraft industry has raised interest in using magnesium alloys to replace aluminum alloys in some structural and mechanical parts. Indeed, magnesium alloy densities are 36% lower than aluminum alloys, leading to a high strength to weight ratio (180 kN m/kg, comparable with that achieved in aluminum alloys). Magnesium alloys are also attractive owing to their electromagnetic interference shielding properties and their recyclability. However, magnesium alloys present low hardness and wear resistance, and adhesion or seizing phenomena easily occur with the opposed materials, when friction is happening. One of the most effective ways to prevent an untimely adhesive and abrasive wear is to harden the surface.

In the previous years, the laser treatment was already employed to improve wear properties of titanium [1] and aluminum alloys [2]. However, the research in the field of laser surface treatment of magnesium alloys to prevent wear is limited and this field is still under development.

Galun et al. published one of the first contributions about the improvement of magnesium alloy wear properties by laser surface treatment. The authors have investigated the feasibility of laser surface alloying of some Mg base alloys with Al, Cu, Ni and Si and different combinations of these elements [3,4]. In all cases the laser alloying process led to an increase of hardness caused by the formation of intermetallic compounds. This resulted in improved wear resistance and in some cases additionally in improved corrosion resistance.

Dutta Majumdar et al. have performed the laser surface alloying of MEZ[1] magnesium alloy with SiC powder [5] or Al+Al$_2$O$_3$ [6] powders. In another work, the same authors studied the effect of a laser surface melting on wear resistance of the MEZ alloy [7].

Laser surface alloying of AZ91[2] with Si, SiC, TiC and Ni, (Al and Si) is reported to enhance sliding wear resistance of the alloy [8–10].

As can be seen, the studies on this subject are not numerous and often come from the same authors. In addition, most of the work concerned primarily with the process of surface treatment (laser parameters, injected powder, etc.). On surface properties, these studies compare mainly the wear loss of the as-received magnesium alloy and the same following laser surface modification. In most of cases, the superior wear behavior of laser surface modified layer is attributed to improved microhardness in the surface layer because of the presence of hard phases. The grain refinement in the treated area is also referred to as probable factor of improved wear resistance [7]. In these works, the authors provide little explanation of the wear mechanisms. Some point to the possibility that these mechanisms are complex and include adhesion, surface and abrasive wear [11].

In this investigation, the effect of laser surface alloying of commercial ZE41 magnesium alloy using Al12%Si powder on tribological properties is studied. A special effort is made to try to understand the mechanisms involved in friction and wear behavior.

---

* Corresponding author. Tel.: + 33 442938198.
 E-mail address: agnes.fabre@ensam.eu (A. Fabre).

[1] MEZ is a magnesium alloy with 2% rare earths, 0.5% Zn, 0.1% Mn and 0.1% Zr.
[2] AZ91 is a magnesium alloy with 8–10% Al, 0.35–1% Zn and 0.13–0.15% Mn.

2. Experimental

2.1. Materials

The base material is a RZ5 commercial magnesium alloy (ASTM ZE41) produced by Honsel Foundry GMB, whose nominal composition is described in Table 1. Fig. 1 is a scanning electron micrograph of the microstructure of ZE41-T5. The micrograph shows an equiaxed grain structure of α-Mg consistent with cast plate, with a grain size about 50–150 μm. A second phase is clearly visible at the grain boundaries. It contains a main quantity of zinc and rare earths (RE: lanthanum and cerium) and has been identified as Mg_7Zn_3RE [11]. Zirconium is dissolved in the α-Mg matrix. The measured value of Vickers microhardness is about 70 $HV_{0.050}$.

The surface laser alloying was performed using Trumpf YAG laser HL3006D in the "Laboratoire Laser et Traitements des Matériaux" of Bourgogne University (France). The laser beam was transmitted at the interaction zone by an optical fiber with an inside diameter of 600 μm. Since nozzle diameter was selected as 4 mm, we also adapted the circular laser spot to 4 mm for a better coupling effect between the powder stream and the laser beam. Fiber output, the laser beam occurs in the form very close to a Gaussian beam.

Al–Si powder (12 wt% of Si) deposition and melting was done with a power of 1500 W, on a ZE41-T5 substrate. Beside the as-cast substrate from magnesium alloy, a surface treatment (conversion treatment) was applied, in order to have a better coupling efficiency between the laser beam and the substrate. The working parameters to obtain a single-layer coating have been established through an experimental design. The working parameters that led to the best results in single-layer coating process constituted the start point for the multi-layer coating process. Five consecutive passes were performed with increasing speed (300 mm/min for the first pass, 400 mm/min for the second and the third and 500 mm/min for the two last). The laser speed was increased from pass to pass in order to take into account of the sample heating during previous passes. The details of laser processing can be found in Ref. [12].

Due to the heat diffusion inside the substrate, the coat layers height is not constant on layer's length. The samples were machined to achieve flat surface and polished. The samples were cut perpendicularly to the laser feed direction and mechanically polished. The surfaces were cleaned with rectapur alcohol. Microstructure analysis and hardness characterization were performed on cross-section of as-cast and laser treated samples. The microstructure observations were conducted after 4%-Nital etching. The scanning electron microscopy observations (SEM) and the chemical composition were obtained by using JEOL 6400 scanning electron microscope (accelerating voltage 20 kV and working distance 25 mm) coupled with an Oxford INCA X-ray microanalysis system or dispersive energy spectrometer (EDX).

The Vickers microhardness measurement on the cross-section was determined for a load of 0.49 N on the base metal and on the coat layer.

2.2. Friction tests

Friction dry tests were carried out on a ball-on-flat tribometer with a straight reciprocating motion. The experiments were performed in air, at room temperature and atmospheric pressure. The ball consists of 14 mm diameter AISI 52100 steel, chemical compositions are given in Table 1. The flat sample was polished: the value of roughness, Ra is about 0.04 ± 0.02 μm. The arithmetic roughness of the ball, Ra, was less than 0.125 μm. The surfaces were cleaned with alcohol rectapur before the beginning of the tests. The test conditions are defined in Table 2: on one cycle, the sliding distance is 20 mm (10 mm forward and 10 mm backward stroke), 2 replicate tests per condition were done. Friction coefficient was continuously recorded during test. The shape of wear zone was determined using Surfascan 3D stylus profilometer with a 10 μm tip radius: three profiles were measured transversally to the sliding direction on the flat samples. The area of the wear zone was characterized using the cross-section profile. Wear volume indicator is defined by the product of this value by the stroke about 10 mm. The wear rate is calculated using the wear volume divided by the sliding distance.

3. Results and discussion

3.1. Coat structure

The coat is composed by five overlapping clads with a little more than 1.8 mm depth of penetration into the base material.
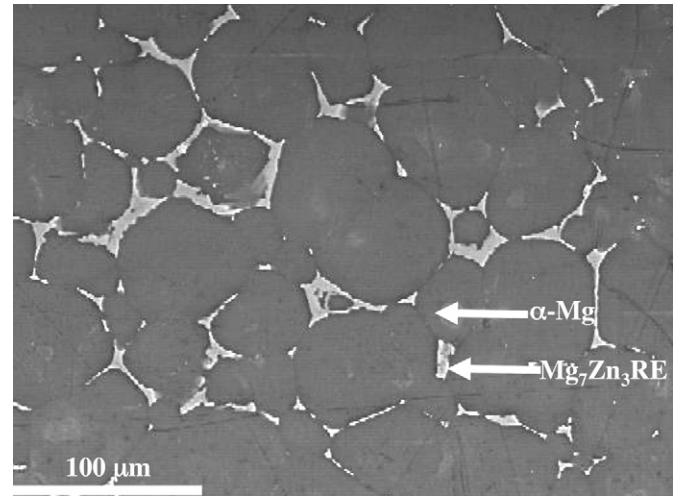

Fig. 1. Scanning electron micrograph of ZE41-T5.

Table 2
Tribological test conditions.

Load	1.9 N
Counterpart	14 mm diameter steel ball, AISI 52100 steel
Contact geometry	Ball-on-flat
Motion	Unidirectional reciprocating
Motion amplitude	10 mm
Motion frequency	1 Hz
Ambient temperature	23 °C (average)
Number of cycles	10, 100, 200, 800, 1000, 3000 and 6000 cycles

Table 1
Chemical composition of the ZE41 magnesium alloy and the AISI 52100 ball steel (in wt%).

Material	Zn	RE	C	Zr	Mn	Si	Fe	Cu	Mg	P	S	Cr
ZE41 Magnesium alloy	3.21	1.23		0.83	0.013	0.009	0.007	0.004	Balance			
AISI 52100 steel			0.95–1.05		0.25–0.45	0.15–0.35	Balance			0.03 max	0.025 max	1.35–1.65
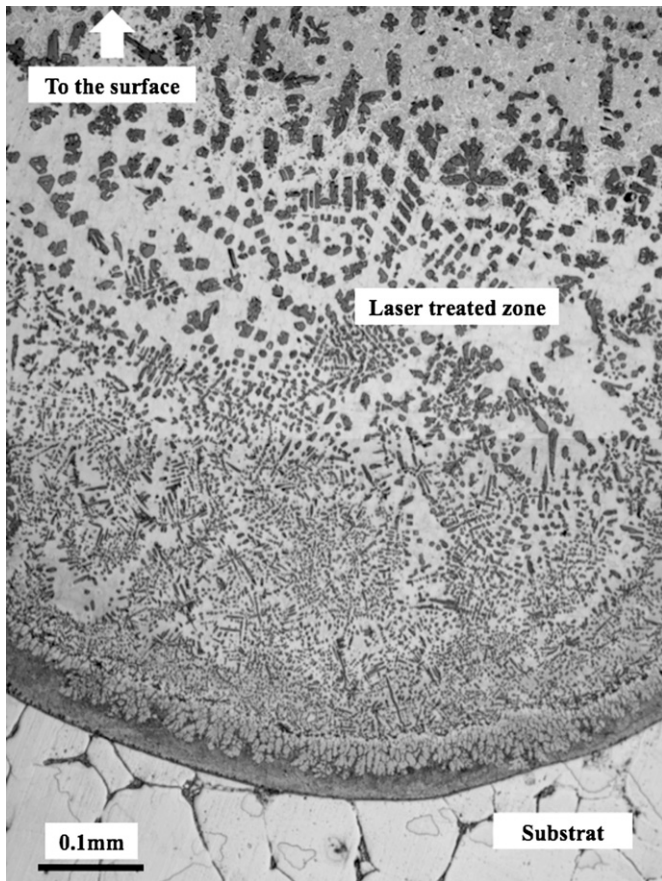
Fig. 2. Optical micrograph of sample cross-section laser treated.

Fig. 3. SEM micrographs of melted zone (a) beneath surface and (b) dendrites in laser clad layer.

The general coat macrostructure obtained is similar to the Al powder laser cladding of the same alloy described in [12]. There were no pores, either on the surface layer or at the interface between surface layer and base metal. The coat layer presents a very good bond aspect. The link between the deposited and the base alloy materials is a very solid and uniform one. Fig. 2 shows a typical example of the microstructures found in transverse cross-sections of the alloyed tracks. It can be observed that three different zones with microstructure varied from the original base material, throw the interfacial heat-affected zone (HAZ) to the solidified melt, which has a complex microstructure with a great number of precipitates. No grain coarsening within the heat-affected zone was observed. But a liquation of the grain boundaries adjacent to the fusion boundary was observed in the HAZ. The melting of some low melting point intermetallics at grain boundaries caused this. For the matrix, Al, Mg, Al_3Mg_2 and $Al_{12}Mg_{17}$ phases are detected by X-ray diffraction analysis, in complement of Mg_2Si dendrites. Al-rare earths were detected only on the HAZ, more than 1 mm beneath the surface.

At the bottom of clad layer, solidification started by epitaxial growth from the partially molten magnesium grains (Fig. 2). A specific microstructure is observed combining dendrites as well as squares or rectangles (Fig. 3) and (Al and Mg) matrix. The chemical composition and the crystal structure were determined by EDX analysis and TEM microdiffraction in a previous work [13]. Dendrites are formed by equilibrium fcc Mg_2Si phase. Nevertheless, high stability and easy formation of Mg_2Si phase are confirmed by thermodynamic calculations. In previous study, some interesting features for tribological behavior are observed on the microstructure: the dendrites size decreases with the increase of the laser pass speed, but their surface fraction in the
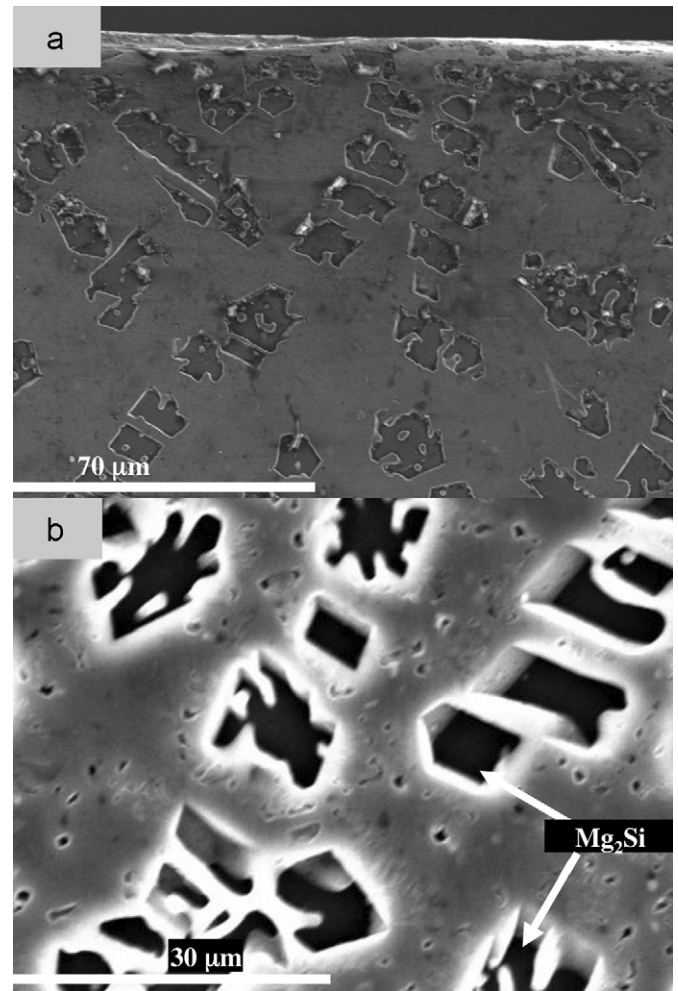
solidified melt stays about $22 \pm 4\%$ for all coats. Beneath the surface from the top to 100 μm in-depth, range size of Mg_2Si dendrites is about 4–50 μm.

In the base material, Zn was detected in a second phase at grain boundaries. In the treated area, Zn was detected in the matrix. This is also the case for rare earths. These elements stay mainly at the interface between the melted layer and the base material. This effect may be attributed to the low diffusion coefficients and the formation of very stable refractory binary compounds with Al that precedes even the formation of $Mg_{17}Al_{12}$-phase. Zr, dissolved in the α-Mg in base material, is found in the coated area in the form of precipitates. In previous work, we identified these precipitates as Al_3Zr [13].

3.2. Microhardness measurements

In-depth microhardness values are presented in Fig. 4. The stable microhardness value in the coating zone, from the top to 1.2 mm in-depth is near 230 $HV_{0.050}$. At 1.65 mm in-depth, near the interface zone between layer and substrate, microhardness reaches a maximal value about 291 $HV_{0.050}$. All these values are high for Al or Mg alloys, and for the ZE41 as-cast alloy, which hardness is about 70 $HV_{0.050}$. The Vickers microhardness of Mg_2Si phase was evaluated at 450 HV in agreement with literature [14]. The evolution of hardness is explained by the contribution of the hard dendrites Mg_2Si. Moreover, combining with the presence of Al-rare earths precipitates, smallest size of the Mg_2Si dendrite,
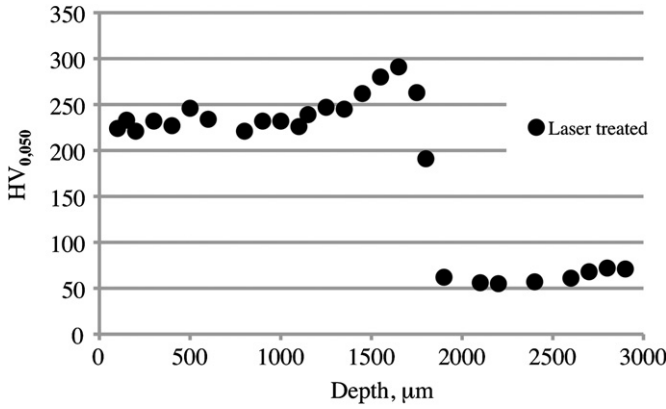
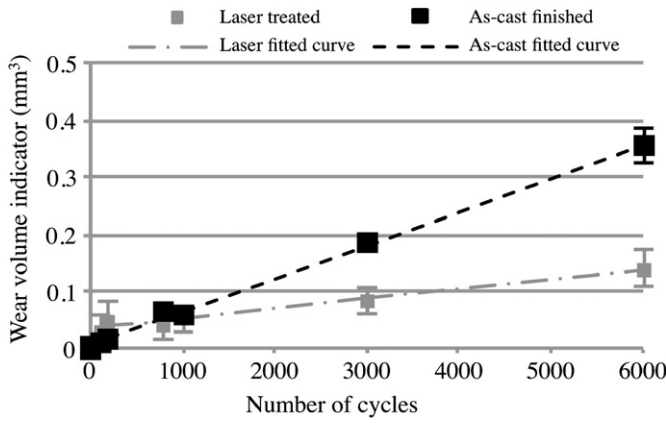Fig. 4. Microhardness profiles along laser treated sample in a cross-section.

Fig. 5. Wear test results.

involves an increase of the maximum hardness value at the interface between layer and substrate [13].

3.3. Wear and friction results

Fig. 5 allows us to compare the wear volume indicators after friction tests: analyses were conducted after tests of 10–6000 cycles. For short tests, values of wear volume indicator seem to be higher for the laser treated samples than those obtained for as-cast ZE41 samples. The wear process seems to be the same for the both types of samples: with an accommodation of the tribological system between 1 and 200 cycles of friction, in the case of laser treated ZE41. It seems happening only for few cycles, no more than 100, after test begin for ZE41. In this case the strong increase of wear informs about the accommodation of the contact zone in the friction system.

After the tests between 200 and 6000 cycles of friction, values of wear volume indicator present a linear evolution with the raise of the number of cycles: smaller slope, characterizing a stable wear regime. In Fig. 5, for as-cast ZE41 and laser treated ZE41, results are fitted by linear curves. Profiles of wear tracks on magnesium alloy samples have demonstrated that as-cast ZE41 surfaces wore much faster than laser treated samples after 1000 cycles of friction.

The precise value of normalized wear rate is defined by the quotient of the wear volume by the sliding distance. The mean value is close to 3.2×10^{-3} mm^3/m for the tests of 800–6000 cycles on the as-cast samples. This value is quite similar for the tests of 800–1000 cycles on the laser treated samples. But after 1000 cycles of friction this value decreases considerably to 1.2×10^{-3} mm^3/m, value obtained for the 6000 cycle's test. The wear rate for the test of 6000 cycles of fiction is noted wr_{6000} in
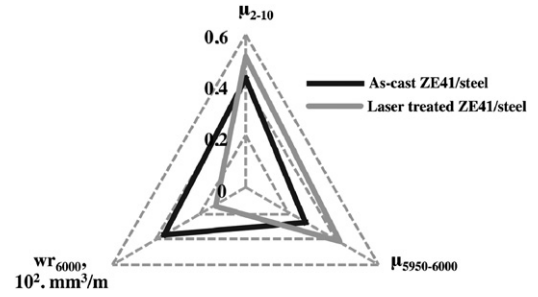

Fig. 6. Friction coefficients and wear rate: μ_{2-10}, average for the first 10 cycles, $\mu_{5950-6000}$, average for the last 50 cycles, wr_{6000}, wear rate after the test of 6000 cycles.

Fig. 6. It is clear that the surface of as-cast ZE41 sample presents no big wear resistance: lower than 2.5 times that of the laser treated ZE41. The microhardness value of as-cast ZE41 is lower than 3.3 times that of the laser treated ZE41.

It is difficult to compare these results with the results obtained by Anbu selvan and Ramanathan in [15]. The wear rate on ZE41A is 2.4×10^{-5} mm^2 for sliding speed about 0.05 m/s and 120 N for load. This result is seven more times over than the result obtained in this current study after 6000 cycles of friction. Even if the hardness value for this magnesium alloy and the counterface steel are close to the values of ZE41 and AISI 52100 steel in current study, the conditions of test are significantly different: the pin-on-disk motion is continuous, with a plane contact zone in Anbu selvan's study. The levels of the mean pressure are different in these two cases. Effectively, the mean value of the contact pressure on ZE41A during the test of wear is about 4 MPa for the Anbu selvan's study. In our current study this value is about 150 MPa.

In conclusion, for the current study, the laser treatment improves significantly the wear resistance: the wear rate of as-cast material is 2.5 times higher than that of the laser treated ZE41. A similar improvement of wear resistance is analyzed on AZ91D due to the Mg$_2$Si formation in the clad layer in [16]: for the resistance of the surface layer, an increase more than 3 times that of the AZ91D is obtained for a sliding distance about 100 m.

Kinetic friction coefficients were recorded during the tests. Complementary tests were done on roughing milled surface, the roughing and finishing milling as-cast ZE41 materials exhibited essentially the same steady-state friction coefficient (0.27), which is about half observed for the laser treated samples (0.43) after 6000 cycles. In Fig. 6, the steady-state friction coefficient, $\mu_{5950-6000}$ is defined by the average of values recorded between the 5950 and 6000 cycles. The friction coefficient in the beginning of the test is noted μ_{2-10} in Fig. 6. The value is lower for as-cast sample than the value for laser treated sample (0.43 and 0.51).

In order to explain the wear process, analysis is conducted on the friction coefficient. Examples of friction coefficient evolution are presented in Fig. 7 for the steel ball sliding on the as-cast sample. In Fig. 7(a), the average value oscillates between 0.27 and 0.28, after 100 cycles until 6000 cycles. This value decreases slowly to the last value near 0.27. After the 20 first cycles, the friction behavior seems to be regular all along cycles between the cycle 22 and 6000. In Fig. 7(b), a main evolution can be observed on the first 20 cycles: after that stabilization appears near to the value 0.3. The accommodation contact zone seems to be realized in the 20 first cycles. The third body appears quickly after few cycles of friction. Some debris is ejected out of the sliding zone because of the reciprocating motion. Wear on the as-cast sample, then, seems to be regular to product third body in order to generate a weak friction coefficient: the accommodation of sliding speed between the ball and the sample on the contact zone is surely done by the movement of the grains of third body.
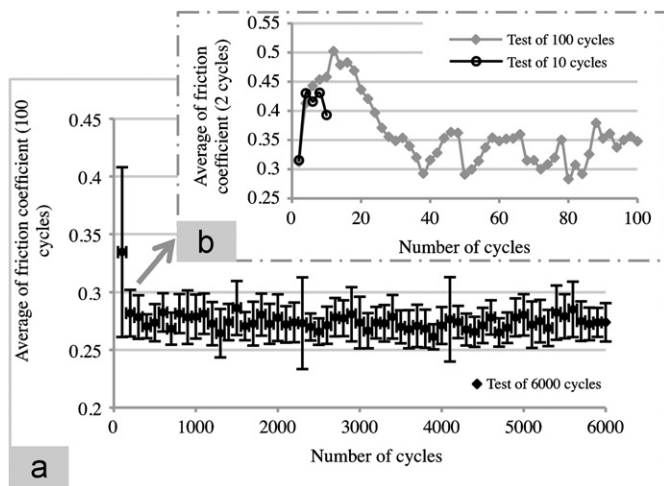
Fig. 7. Friction coefficient evolution: as-cast ZE41 (a) average values for 100 cycles on the test of 6000 cycles and (b) average value for 2 cycles on the test of 100 cycles.
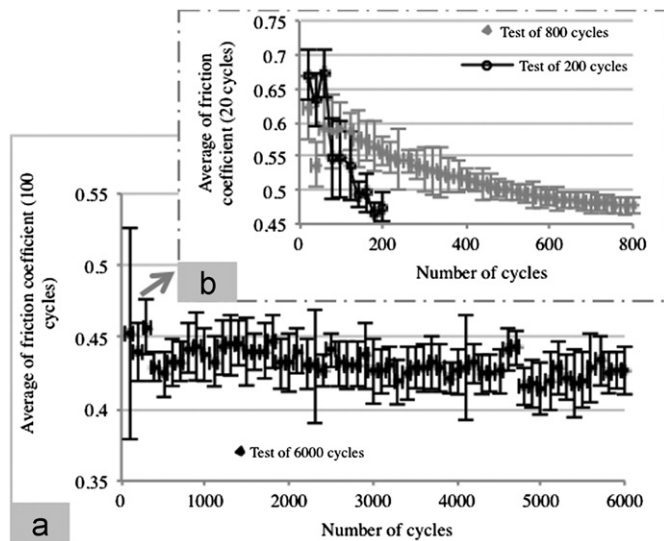

Fig. 8. Friction coefficient evolution: laser treated ZE41 (a) average values for 100 cycles on the test of 6000 cycles and (b) average value for 20 cycles on the test of 200 cycles.

Due to the creation of the third body, the modification of the tribological system induces an accommodation between the two solids, in term of velocity. The sliding between the two solids is changing in a rolling between the third body and the solids.

In Fig. 8(a), the oscillate value of friction coefficient can be observed between 0.4 and 0.45 for 200–6000 cycles for laser treated sample: the average value, $\mu_{5950-6000}$ is equal to 0.43. In Fig. 8(b), the stabilization of the friction coefficient seems to be over 200 cycles. In these cases, the kinetic of accommodation is slowly in front of the as-cast sample. Longer time seems necessary to adapt the contact zone.

In all cases, a transfer effect took place between the sample and the ball: microscopic observations and chemical analysis showed Mg and alloying elements particles on the steel ball surface. On as-cast samples, particularly, Mg element was found on steel ball after the test of 10 cycles. The weight% of Mg and O increases with the raise of the number of friction cycles, as it is shown in Table 3. On the ball of the test of 100 cycles, some zinc is found. For as-cast adhesive wear is activated quickly on the first cycles of friction, that means the wear mechanism quickly moves into the adhesive wear regime.

Table 3
Main components in the transfer layer on the steel ball, in weight%, for different tests of friction against as-cast ZE41, or against laser treated ZE41.

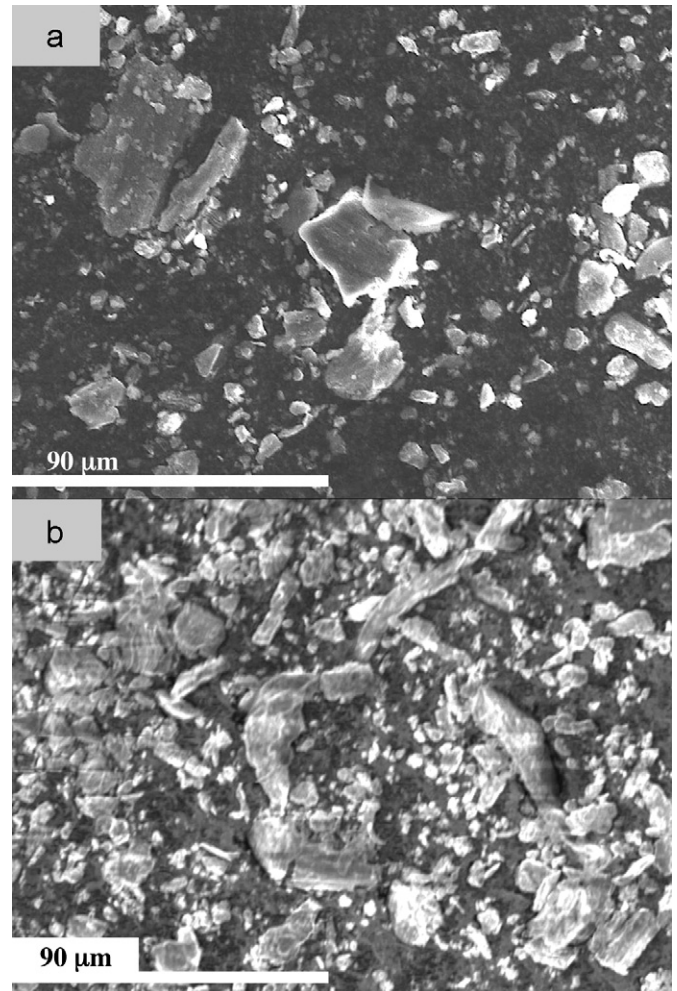| Chemical component		Mg, weight%	O, weight%	Al, weight%
On steel ball/as-cast ZE41	After 10 cycle's test	9.3	0	0
	After 100 cycle's test	28	5.6	0
	After 800 cycle's test	27.9	11.6	0
	After 6000 cycle's test	29.9	15.6	0
On steel ball/laser treated ZE41	After 200 cycle's test	3.2	9.3	10.8
	After 800 cycle's test	6	6.3	20.8
	After 6000 cycle's test	5.1	7.3	23.8

Fig. 9. Morphology of debris after test of 3000 cycles (a) as-cast ZE41/steel and (b) laser treated ZE41/steel.

On the laser treated samples, chemical analysis showed a presence of Mg, O and Al after the test of 200 cycles on the ball. In this case, the weight% of Al increases for the longer tests. For the laser treated surface, adhesive wear is activated.

In the two cases, adhesion is the same mechanism of wear; nevertheless, the transfer components are different.

In all the tests, third body is created. Some investigations are conducted on the debris obtained after the 3000 cycles. SEM images are shown in the morphology of debris, in Fig. 9(a), debris obtained after friction with magnesium alloy against steel seem to be larger, and with appearance of shape more rectangular than the debris produced by friction between laser treated surface

magnesium against steel, in Fig. 9(b). Table 4 presents result of chemical analysis. In the as-cast ZE41/steel sliding, debris is mainly composed by Mg and O. In the laser treated ZE41/steel sliding, debris essentially contains Al and O. But with the value of Mg (10.2%) is twice much more than the Si one (4%), the Mg_2Si seems to be logically present. Maybe the Al component moderates effect of hard debris, avoiding large grooves on the laser treated sample, however Mg_2Si debris presents a very high microhardness values (450 HV). This effect combining with the hardened effect on the surface, after laser treatment, increases significantly wear resistance. In table 5, the highest level of weight% of O is observed on the smaller debris samples (maximum dimension less than 10 μm) in comparison with those having a maximum dimension greather than 20 μm. The results are opposed for weight% of Al. These average results are obtained on four debris, the standard deviation is no more than 3%. The high level of O on small debris can be linked with the time of debris staying in contact zone. Maybe larger debris is quickly ejected from the contact zone. More investigations are to be conducted in order to understand if Al and O present a main influence on the wear

resistance: in particular if it decreases hardness of the debris and if there is a specific morphology of debris.

In Fig. 10, SEM observation on the flat samples, in the sliding zone after the tests of 6000 cycles show some parallel grooves and ridges as a scuffing effects: the width of grooves are more large for as-cast ZE41, in Fig. 10(a) than that of the laser treated one, in Fig. 10(b). The same effect is observed on the transfer zone on the balls after tests of 3000 cycles, Fig. 10(c) for ball/as-cast ZE41 friction test and (d) for ball/laser treated ZE41 friction test. The thickness of the transfer layer is not constant: then, the abrasive process seems to be combined with the adhesive wear.

Table 6 presents the difference between values of weight% for Mg, O, Si, Al and Zn components detected by EDX analysis in the wear scar and out the wear scar for the two surfaces of as-cast and laser treated ZE41 samples after the tests of 6000 cycles. These results show the presence of O for as-cast ZE41 and laser treated surface samples in the wear zone, as well on the transfer layer (Table 3) and on the debris (Fig. 9) such as an oxidation mechanism effect. This was observed on the literature [16,17],

Table 4
Chemical components, in weight%, on debris after 3000 cycles of friction for as-cast ZE41/steel and laser treated ZE41/steel tests.

Chemical component	Mg, wt%	O, wt%	Al, wt%	Si, wt%	Zn, wt%
Debris as-cast ZE41/steel	54.7	43.3	0	0	2
Debris laser treated ZE41/steel	10.2	45.2	40	3.9	0.7

Table 5
Chemical components, in weight%, on small and large debris after 3000 cycles of friction for laser treated ZE41/steel tests.

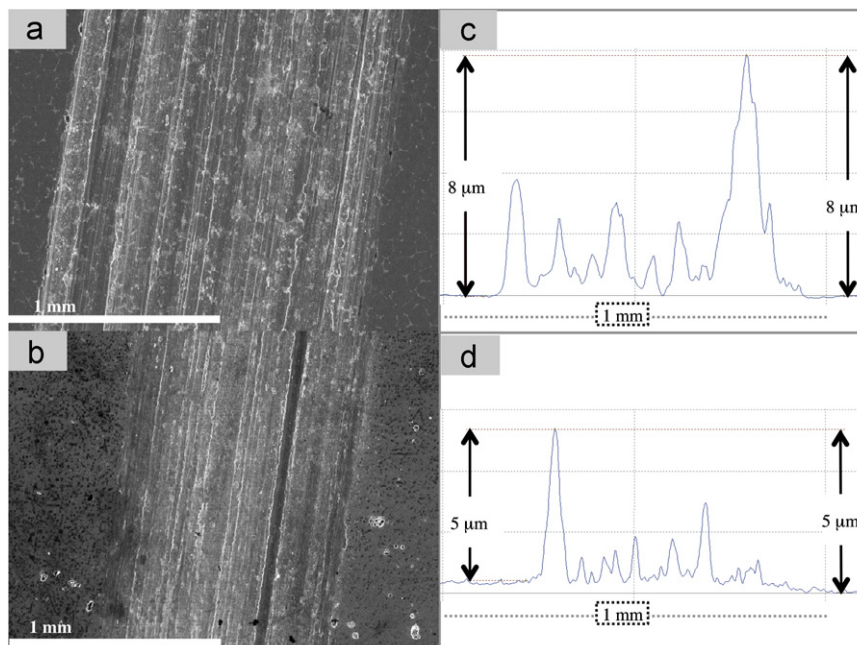| Chemical component	Mg, wt%	O, wt%	Al, wt%	Si, wt%	Zn, wt%
Small debris laser treated ZE41/steel	9.1	48	38	3.9	1
Large debris laser treated ZE41/steel	14	14.9	62.5	7.4	1.2

Fig. 10. Wear zone after the test of 6000 cycles for (a) as-cast ZE41 sample, (b) laser treated ZE41 sample. Profile of transfer layer after the test of 3000 cycles, for (c) ball against as-cast ZE41 and (d) ball against laser treated ZE41.

Table 6
Difference between values of weight% in the wear scar and out the wear scar for the two surface of as-cast and laser treated ZE41 samples after the tests of 6000 cycles.

Chemical component	Mg, wt%	O, wt%	Al, wt%	Si, wt%	Zn, wt%	Zr, wt%
As-cast ZE41/steel	−7.5	8.4	0	0	−0.9	0
Laser treated ZE41/steel	−2.3	25	−20.3	−2.2	−0.2	0

and described such as the mild wear effect: magnesium oxide created under thermal loading due to caloric dissipation of friction energy combining with containment zone in the contact.

In conclusion, the wear behavior of coating surface is attributed to improve microhardness in the modified surface layer as compared to untreated material: the hardness is 3.3 times higher linked to the wear resistance, which is 2.5 times higher. The Mg_2Si, which involves a hardness of the treated sample, is present in debris. Nevertheless, a limitative abrasive effect of this debris is observed conducting to a wear reduction.

Other study will be conducted in order to investigate the relationship between the size of Mg_2Si dendrites and the wear rate. With adapted conditions of treatment, the capability of laser cladding to produce precise size of dendrites maybe an advantage to optimize the wear resistance of the laser surface alloying.

4. Conclusions

The microstructure and wear behavior of commercial alloy ZE41 modified by surface laser alloying with Al–Si powder mixture were studied. The coating is mainly composed of an Al–Mg matrix and dendrite precipitates of Mg_2Si. Laser alloying process led to an increase of hardness with an improved microhardness, about 230 $HV_{0.050}$, close to the surface, as compared to the 70 $HV_{0.050}$ of the as-received substrate, caused by the formation of intermetallic compound Mg_2Si.

The surface modification by laser cladding involves microstructural properties that increase the friction coefficient against AISI 52100 steel counterface: the steady-friction coefficient is about 0.45 (0.27 for ZE41/AISI 521000 steel).

Nevertheless, the results indicate in increase wear resistance of laser treated parts more than 2.5 times that of the as-cast ZE41.

These results have given new information for the wear resistance of laser treated surface ZE41 with Al12Si% powder in the case of low sliding speed and high level of pressure. The wear is due to adhesive and abrasive mechanisms, which seem to be combined with oxidation process.

References

[1] Tian YS, Chen CZ, Li ST, Huo QH. Research progress on laser surface modification of titanium alloys. Applied Surface Science 2005;242:177–84.

[2] Fu Y, Batchelor AW. Laser alloying of aluminium alloy AA 6061 with Ni and Cr. Part II. The effect of laser alloying on the fretting wear resistance. Surface and Coatings Technology 1998;102:119–26.

[3] Galun R, Weisheit A, Mordike BL. Surface alloying of magnesium base alloys with high-power CO_2-laser. Proceedings of SPIE 1997;3092:744–7.

[4] Kutschera U, Galun R. Wear behaviour of laser surface treated magnesium alloys. In: Kainer KU, editor. Magnesium Alloys and their Applications. Weinheim: Wiley-VCH Verlag GmbH; 2000 pp. 330–5.

[5] Dutta Majumdar J, Ramesh Chandra B, Galun R, Mordike BL, Manna I. Laser composite surfacing of a magnesium alloy with silicon carbide. Composites Science and Technology 2003;63(6):771–8.

[6] Dutta Majumdar J, Ramesh Chandra B, Mordike BL, Galun R, Manna I. Laser surface engineering of a magnesium alloy with $Al+Al_2O_3$. Surface and Coatings Technology 2004;179:297–305.

[7] Dutta Majumdar J, Galun R, Mordike BL, Manna I. Effect of laser surface melting on corrosion and wear resistance of a commercial magnesium alloy. Materials Science and Engineering A 2003;361:119–29.

[8] Hiraga H, Inoue T, Kojima Y, Kamado S, Watanabe S. Surface modification by dispersion of hard particles on magnesium alloy with laser. Materials Science Forum 2000;350:253–8.

[9] Murayama K, Suzuki A, Takagi T, Kamado S, Kojima Y, Hiraga H. Surface modification of magnesium alloys by laser alloying using Si powder. Materials Science Forum 2003;419–422(II):969–74.

[10] Dutta Majumdar J, Manna I. Mechanical properties of a laser-surface-alloyed magnesium-based alloy (AZ91) with nickel. Scripta Materialia 2010;62(8):579–81.

[11] Neil WC, Forsyth M, Howlett PC, Hutchinson CR, Hinton BRW. Corrosion of magnesium alloy ZE41-the role of microstructural features. Corrosion Science 2009;51(2):387–94.

[12] Ignat S, Sallamand P, Grevey D, Lambertin M. Magnesium alloys (WE43 and ZE41) characterisation for laser applications. Applied Surface Science 2004;225:124–34.

[13] Volovitch P, Masse JE, Fabre A, Barrallier L, Saikaly W. Microstructure and corrosion resistance of magnesium alloy ZE41 with laser surface cladding by Al–Si powder. Surface and Coatings Technology 2008;202(20):4901–14.

[14] Lü Y, Wang Q, Zeng X, Ding W, Zhai C, Zhu Y. Effects of rare earths on the microstructure, properties and fracture behavior of Mg–Al alloys. Materials Science and Engineering A 2000;278:66–76.

[15] Anbu selvan S, Ramanathan S. Dry sliding wear behavior of as-cast ZE41A magnesium alloy. Materials and Design 2010;31:1930–6.

[16] Yang Y, Wu H. Improving the wear resistance of AZ91D magnesium alloys by laser cladding with Al–Si powders. Materials Letters 2009;63:19–21.

[17] Lim CYH, Lim SC, Gupta M. Wear behaviour of SiCp-reinforced magnesium matrix composites. Wear 2003;255:629–37.